A Study on Prediction of the Base Pressures for an Axi-Symmetric Body

Doo-Sung Baik*, Young-Chool Han

Graduate School of Automotive Engineering, Kookmin University, 861-1, Chongnung-dong, Songbuk-gu, Seoul 136-702, Korea

A flow modeling method has been developed to analyze the flow in the annular base (rear-facing surface) of a circular engine nacelle flying at subsonic speed but with a supersonic exhaust jet. Real values of exhaust gas properties and temperature at an altitude of 30, 000 feet are employed. Potential flows of the air and gas streams are computed for the flow past a separated wake. Then a viscous jet mixing is superimposed on this inviscid solution. Conservation of mass, momentum and energy for the wake flow field is achieved by multiple iterations with modest computer requirements.

Key Words : Base Flow, Nacelle, Base Pressure, Viscous, Inviscid, Turbulent

Nomenclature

c_p : Specific heat
C_p : Pressure coefficient
C_r : Crocco number, U/U_{max}
D : Distance the body extends upstream from the base
E : Distance of the downstream from re-combination point
$E(k)$: Second elliptical integral
h : Enthalpy
H : Height of the base
$K(k)$: First elliptical integral
L : Length wake extends from the base
P : Pressure
Pr : Prandtl number
R : Radius from nacelle axis
R_i : Radius of computation ring
R_j : Radius of singularity ring
$\Re$: Gas constant
T : Temperature
U, V : Velocity components
x, y : Coordinates fixed to the jet mixing region
X,R : Axi-symmetric coordinates
X, Y : Reference inviscid coordinates
X_o : Axial distance of virtual origin from separation point
Y_o : Normal distance of virtual origin from coordinates fixed to the jet mixing region
y_m : Shift of x-axis from X-axis
α : Mach angle $(=\sin^{-1}(M^{-1}))$
β : $=\sqrt{1-M_\infty^2}$
γ : Ratio of specific heats; vortex strength
δ : Boundary layer thickness
δ_1 : Boundary layer displacement thickness
δ_2 : Boundary layer momentum thickness
η : Dimensionless y coordinates
θ : Flow angle from body axis
μ : Ring source strength
ρ : Density
σ : Jet mixing spreading parameter
Φ : Velocity ratio, u/U_e
ω : Surface angle from the axis

* Corresponding Author,
E-mail : dsbaik@kmu.kookmin.ac.kr
TEL : +82-2-910-4817; **FAX** : +82-2-910-4718
Graduate School of Automotive Engineering, Kookmin University, 861-1, Chongnung dong, Songbuk-gu, Seoul 136-702, Korea. (Manuscript **Received** January 15, 2001; **Revised** August 1, 2001)

1. Introduction

For decades, there has been considerable interest in understanding and predicting the characteristics of aircraft afterbody flow. In the

beginning of such research, only experimental methods were available. Since the experimental studies could be quite complex and expensive, there has been considerable interest in developing less expensive, yet reliable, analytical and numerical schemes. For the most accurate results, the full Navier-Stokes equations should be solved using a finite difference method, but it requires a large computer and long computational time. Holst (1977) first solved the Navier-Strokes equations for supersonic flows over axisymmetric boattails with a solid plume simulator. Mikhail (1978) removed the solid plume simulator and considered a centered propulsive jet emanating from a sharp lipped nozzle at a Mach number of one. Peery and Forester (1979) treated multistream nozzle flows with transonic external flow and a central jet with the exit area equal to the body area. Deiwert (1980) used an implicit method to simulate subsonic, transonic and supersonic three dimensional separated flows over axisymmetric boattailed bodies with a solid plume simulator. Hasen (1982) obtained the numerical solution for an axisymmetric nozzle in supersonic external flow field using Mac Cormack's method.

All of the above methods used different forms of finite difference techniques. Here a large portion of the enveloping flow field must be computed point by point to find the pressure in a small region, which requires thousands of computational points. Singularity methods require only that the flow conditions on body (or jet) surface be computed.

Korst and Tripp (1957) investigated the base pressure behind a blunt trailing edge for supersonic two-dimensional flow. Two approaching streams on each side of the trailing edge had the same composition, constant specific heats, and identical stagnation temperature, but different Mach numbers and stagnation pressures. Page and Korst (1955) developed the constant pressure free jet mixing of a turbulent supersonic plane backstep flow with supersonic atmospheric flow of the same gas but different total temperature from the wake. Later, Korst's two-stream theoretical base flow analysis was extended to treat base flow on an axisymmetric afterbody with a single operating exhaust nozzle by Dixon and Page (1970). In this both the airflow and nozzle flow were supersonic with same gases.

Prior to Izadi (1991), no work with subsonic outer flow and supersonic inner flow is found despite the frequent occurrence in engine nacelles. Izadi modeled the base region between subsonic and supersonic flows to investigate if a singularity representation could be used with plane geometry, same gas and same total temperature.

For this particular axisymmetric problem, it is essential to have the information about vortex ring and source rings. Unfortunately, the existing venerable theories of this phenomenon are little known, difficult, insufficient, and inconsistent.

The current research development follows the efforts of Izadi, where the base flow due to internal supersonic and external subsonic flows was considered. Furthermore, the propulsion base flow was simplified by the assumptions of two-dimensional flow, air for both flows, and equal total temperatures. An axisymmetric method of characteristics is used to simulate the supersonic wake region.

In the large body of analytical and computational work done on the base flow, one commonly occurring case seems to have been overlooked: an axisymmetric aircraft nacelle with a hot supersonic exhaust gas jet interacting with a subsonic external flow of atmospheric air. This may occurs in several different ways: some are shown in Fig. 1(a) and (b).

In Fig. 1(a), airflow separates from a boattail due to an adverse pressure gradient, creating an annulus. In Fig. 1(b), separation is caused by termination of the exterior surface. The time during which this occurs may be short, but the area on which base pressure prevails is large. Cooling airflow may be added to the annulus in Fig. 1(a) and (b) especially for turbojets with afterburners.

A flow modeling approach, rather than a finite difference method, was used to produce a economical solution in computational time to be useful for aircraft design. Singularities are used for inviscid/subsonic airflow and the axisy-

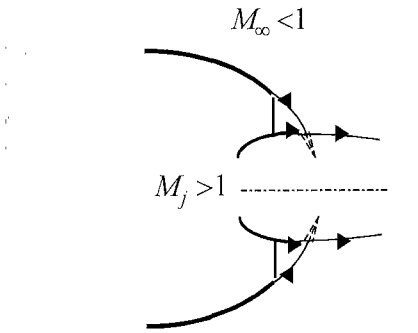

(a) Circular arc boattail nacelle

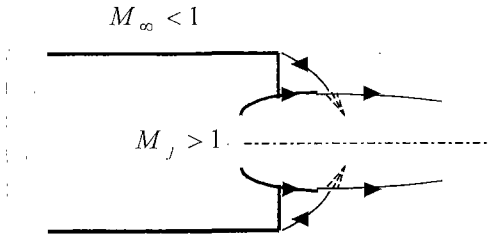

(b) Cylindrical nacelle

Fig. 1 Typical occurrence of axi-symmetric base flows

mmetric method of characteristics is used for supersonic flow. It is possible to specify realistic gas properties. Viscous boundary layers and viscous jet interactions are added to the produced potential flows using the Chapman-Korst jet mixing method.

2. The Model

The mathematical model involves an interactive solution between an outer, inviscid, potential flow and an inner, viscous flow in the near wake. The outer flow includes the subsonic airflow and the supersonic engine exhaust. These flow around the solid nacelle and the base wake. The inner solution then imposes viscous jet mixing and re-circulation flows on the external flow. Satisfaction of mass, momentum and energy conservation is achieved by interactive adjustment of the two flows.

It is typical of flow modeling methods to use knowledge of physical behaviors to simplify the analysis. Prandtl was perhaps the master of this when he proposed the boundary layer in which terms were eliminated on the basis of relative

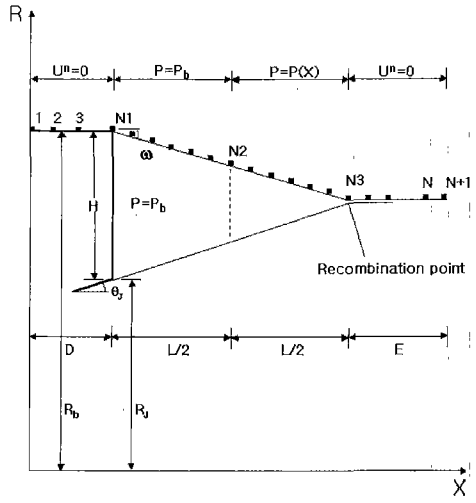

Fig. 2 Boundary conditions representation on body and wake

magnitudes and regions were labeled inviscid or viscous. Similarly, the pressure field patterns for separating-and reattaching flow can be seen in many measured flows.

2.1 Outer flow model

The subsonic potential flow is produced by adding the perturbations due to ring sources and vortices to the atmospheric free stream. The flow is transformed to the incompressible plane for solution, then transformed back to the compressible plane.

Goethert's rule (Shapiro, 1953), where the dot denotes the incompressible case, is as follows (Fig. 2).

$$\dot{X}=X$$
$$\dot{\omega}=\beta\omega$$
$$C_p=\frac{1}{\beta^2}\dot{C}_p$$
$$U_\infty=\dot{U}_\infty$$

where

$$\beta=\sqrt{1-M_\infty^2}$$

Rings were distributed axially and the midpoints between rings were the computation points. The velocities resulting from the free stream and the singularities were added to give the velocity components.

$$\dot{U}_X=\dot{U}_\infty+\dot{U}_{sX}+\dot{U}_{vX}$$
$$\dot{U}_R=\dot{U}_{sR}+\dot{U}_{vR}$$

where (Kuchemann, 1953)

$$\dot{U}_{sX}=\sum_{j=1}^{N+1}\left[\frac{\mu}{2\pi r_j'}\frac{2x}{\sqrt{x^2+(r+1)^2}\{x^2+(r-1)^2\}}E(k)\right]_j$$

$$\dot{U}_{sR}=\sum_{j=1}^{N+1}\left[\frac{\mu}{2\pi r_j'}\frac{1}{\sqrt{x^2+(r+1)^2}}\left[K(k)-\left\{1-\frac{2r(r-1)}{x^2+(r-1)^2}\right\}E(k)\right]\right]_j$$

$$\dot{U}_{vX}=\sum_{j=1}^{N+1}\left[\frac{\gamma}{2\pi r_j'}\frac{1}{\sqrt{x^2+(r+1)^2}}\left[K(k)-\left\{1+\frac{2(r-1)}{x^2+(r-1)^2}\right\}E(k)\right]\right]_j$$

$$\dot{U}_{vR}=\sum_{j=1}^{N+1}\left[\frac{\gamma}{2\pi r_j'}\frac{-x}{r\sqrt{x^2+(r+1)^2}}\left[K(k)-\left\{1+\frac{2r}{x^2+(r-1)^2}\right\}E(k)\right]\right]_j$$

where

$$k^2=\frac{4r}{x^2+(r+1)^2}$$
$$K(k)=\int_0^{\frac{\pi}{2}}\frac{1}{\sqrt{1-k^2\sin^2\alpha}}d\alpha$$
$$E(k)=\int_0^{\frac{\pi}{2}}\sqrt{1-k^2\sin^2\alpha}\,d\alpha$$
$$r=\frac{\dot{R}_j}{\dot{R}_j}$$
$$r_j'=\dot{R}_j$$
$$x=\frac{\dot{X}_j-\dot{X}_i}{\dot{R}_j}$$

The velocity components at a control point i, tangential and normal to the i^{th} surface between rings, can be obtained by means of the following transformation where (is the surface angle:

$$\begin{bmatrix}\dot{U}_i^t\\ \dot{U}_i^n\end{bmatrix}=\begin{bmatrix}\cos\omega_i & \sin\omega_i\\ -\sin\omega_i & \cos\omega_i\end{bmatrix}\begin{bmatrix}\dot{U}_X\\ \dot{U}_R\end{bmatrix}$$

Figure 2 shows the four regions with different boundary conditions to be applied for the outer flow.

i) $1\le i\le N1$

There are (N1) rings over the body, starting at a point upstream (ring 1) having free stream flow and ending at the separating ring (N1). For a control point on this fixed surface, the normal velocities are:

$$\frac{\dot{U}_i^n}{\dot{U}_\infty}=0\quad 0\le X\le D$$

ii) $N1+1\le i\le N2$

For a control point i on the flow surface between (ring N1) and the ring at the mid-distance of the wake (ring N2), the surface velocity at a control points is a function of base pressure.

$$\frac{\dot{U}_i^t}{\dot{U}_\infty}=\beta\frac{U_i^t}{U_\infty}=\beta\frac{U_b}{U_\infty}\quad D\le X\le\left(D+\frac{L}{2}\right)$$

where

$$\frac{U_b}{U_\infty}=\sqrt{1+\frac{1}{M_\infty^2}\frac{2}{\gamma-1}\left[1-\left(\frac{p_b}{p_\infty}\right)^{\frac{\gamma-1}{\gamma}}\right]}$$

iii) $N2\le i\le N3$

For a control point i on the flow surface between the ring (N2) and the ring at the end of the wake (recombination N3), considering an assumption of quadratic pressure rise, the surface velocity at these points are calculated from the following.

$$\frac{\dot{U}_i^t}{\dot{U}_\infty}=\beta\frac{U_i^t}{U_\infty}=\beta\left[\frac{4}{3}\left(\frac{U_{rec}}{U_\infty}-\frac{U_b}{U_\infty}\right)\left(\frac{X}{L}\right)^2-\frac{1}{3}\left(\frac{U_{rec}}{U_\infty}-4\frac{U_b}{U_\infty}\right)\right]$$
$$\text{for}\left(D+\frac{L}{2}\right)\le X\le(D+L)$$

where

$$\frac{U_{rec}}{U_\infty}=\sqrt{1+\frac{1}{M_\infty^2}\frac{2}{\gamma-1}\left[1-\left(\frac{p_{rec}}{p_\infty}\right)^{\frac{\gamma-1}{\gamma}}\right]}$$

iv) $(N3+1)\le i\le N$

Now, considering the rings between the end of the wake and some ring far downstream of the body and assuming that the flow over these rings are parallel to the flow surface, that is, the normal velocity is equal to zero, the surface velocity at the control point of rings is:

$$\frac{\dot{U}_i^n}{\dot{U}_\infty}=0\quad (D+L)\le X\le(D+L+E)$$

Expected pressures are:

$$P_{o\infty}>P_{rec}>P_b$$

The program computes the velocities and changes the wake shape to reduce the normal velocities to zero.

2.2 Jet flow model

Symbols referring to the jet flow are indicated by a prime. The supersonic jet flow is computed by the axisymmetric method of characteristics (Shapiro, 1953), since singularity solutions are

quite difficult for supersonic flow. In addition, the method of characteristics can approach exactness if small increments of control points are used.

The pressure field choices are the same as those made for the subsonic outer flow. The streamlines at the end of the wake should join. If they cross, the chosen base pressure is too low. If they fail to join, the base pressure was chosen too high. A new value of pressures at a base region is chosen and the two calculations repeated until they join at the recombination point.

Downstream of the recombination point, the two streamlines should flow together (parallel) and have the same pressures. If this is not the case, the program moves the streamlines toward to lower pressure side and the two solutions are again calculated with the new downstream geometry. When the wake shapes have relaxed, the upper and lower streamlines meet at a point and flow downstream at the same directions and pressures, and the outer, inviscid computation is completed.

2.3 The inner flow model

The analysis of the viscous flow within the wake is called the inner flow solution. It is based on Korst's turbulent jet mixing theory and base flow analysis. This is modified to include a reverse flowing parallel stream and variable fluid properties. Korst's mixing theory (Korst, 1956), which has strong experimental verification.

Figure 3 displays the jet mixing method. The fully developed velocity profile is shown on the right between two parallel, but opposite flows, U and U_B. The separating flow has a boundary layer. Hill (Hill et al. , 1969) devised a method for representing the effect of the boundary layer on the downstream profile.

He replaced the boundary layer by a virtual starting point for the jet mixing which would have the same displacement and momentum thickness at the actual separation plane as the real boundary layer. This condition leads to an expression.

$$-\frac{\underline{\sigma}}{X_0}\delta_2=\underline{\eta_e}-\underline{\eta_m}-\int_{-\infty}^{e}\frac{\rho}{\rho_e}\underline{\Phi}d\underline{\eta}$$

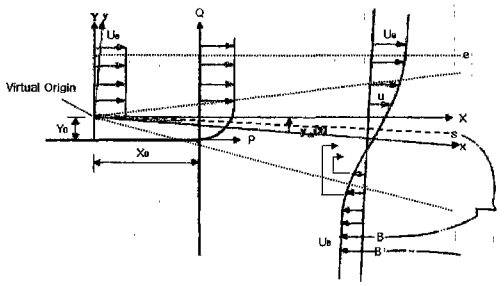

Fig. 3 Basic flow model of the two stream jet mixing

$$=\underline{\eta_e}-\underline{\eta_m}-(1-Cr_e^2)J_{1e} \qquad (1)$$

where

$$J_{1e}=\int_{-\infty}^{e}\frac{\underline{\Phi}}{1-Cr_e^2\underline{\Phi}^2}d\underline{\eta}$$

This location is termed "the virtual origin" whose location is:

$$Y_0=\delta_1+\delta_2 \text{ and } Y_0'=\delta_1'+\delta_2'$$

where δ_1 and δ_1' are displacement thickness, δ_2 and δ_2' are the momentum thickness.

Two coordinate sets originate at the virtual origin. (X, Y) coordinates can be thought of as the edge of the inviscid outer flow. X is parallel to nearby inviscid streamlines, such as e. The (x, y) coordinates belong to the viscous mixing layer. The x coordinate is the center of the jet mixing velocity profile where

$$u=\frac{1}{2}(U_e-|U_B|)$$

The shift of the x coordinate from the X is shown by y_m in Fig. 3.

Korst's theory (Korst, 1956) gives the isobaric, plane turbulent, single stream jet mixing profile as;

$$\underline{\Phi}=\frac{u}{U_e}=\frac{1}{2}(1+erf(\underline{\eta}))\ ;\ \underline{\eta}=\underline{\sigma}\frac{y}{x}$$

$$erf(\underline{\eta})=\frac{2}{\sqrt{\pi}}\int_{-\infty}^{\underline{\eta}}e^{-b^2}db$$

where $\underline{\sigma}$ is the jet spreading parameter and only an empirical value is required. It equals 12 for subsonic flow of many gases and varies with speed for supersonic flow. There is some disagreement among investigators, but the value used here is

$$\underline{\sigma}\cong 12 \text{ for } Cr_e^2\leq 0.255$$

$$\underline{\sigma}=47.1Cr^2 \text{ for } Cr_e^2 \geq 0.255$$

where Crocco number is defined as

$$Cr_e^2=\frac{M_e^2}{\frac{2}{\gamma-1}+M_e^2}=\frac{U_e^2}{2C_pT_o}=1-\frac{T_e}{T_0}$$

For two-stream opposed flows, the single -stream spreading parameter σ is multiplied by

$$\frac{1-\Phi_B}{1+\Phi_B};\ \Phi_B=\frac{|U_B|}{U_e}$$

and the velocity profile is

$$\Phi=\frac{1-\Phi_B}{2}+\frac{1+\Phi_B}{2}erf(\eta)$$

If gases in the two parallel streams have different total temperatures, or if they are different gases and thus have different physical properties, then these vary across the mixing region. If the turbulent viscosity is due to the mixing of gas particles, in the sense of the "exchange coefficient", then the same phenomena transports heat, and mass. Then velocity and total temperature have similar profiles. This says that $p_r=1$.

$$\frac{T_0-T_{0B}}{T_{0e}-T_{0B}}=\frac{\Phi+\Phi_B}{1+\Phi_B}$$

$$\frac{T_0}{T_{oe}}=\left(\frac{\Phi+\Phi_B}{1+\Phi_B}\right)\left(1-\frac{T_{oB}}{T_{oe}}\right)+\frac{T_{oB}}{T_{oe}}$$

In the same way, the exchange of gas globs transports the physical properties of the gases.

$$\frac{\mathfrak{N}}{\mathfrak{N}_e}=\left(\frac{\Phi+\Phi_B}{1+\Phi_B}\right)\left(1-\frac{\mathfrak{N}_B}{\mathfrak{N}_e}\right)+\frac{\mathfrak{N}_B}{\mathfrak{N}_e}$$

and

$$\frac{\gamma}{\gamma_e}=\left(\frac{\Phi+\Phi_B}{1+\Phi_B}\right)\left(1-\frac{\gamma_B}{\gamma_e}\right)+\frac{\gamma_B}{\gamma_e}$$

The non-dimensional density then becomes:

$$\frac{\rho}{\rho_e}=\frac{\mathfrak{N}_e}{\mathfrak{N}}\left[1-\Phi^2Cr_e^2\frac{\gamma_e}{\gamma_e-1}\frac{\gamma-1}{\gamma}\frac{T_{oe}}{T_o}\frac{\mathfrak{N}_e}{\mathfrak{N}}\right]^{-1}\left(\frac{T_{oe}}{T_o}\right)(1-Cr_e^2)$$

and

$$Cr_e^2=1-\frac{T_e}{T_{0e}}$$

The separating streamline, s, separates the mass flowing above the virtual origin from that entrained. The net mass transfer across the separating streamline is zero. The amount of mass flow above the virtual origin remains above the streamline s. Since this is a turbulent mixing region, mass is crossing the line constantly, but net amount crossing is zero. This condition can be written as:

$$\rho_eU_e(y_e-y_m)=\int_s^e\rho u dy \tag{2}$$

After multiplying by $\frac{\sigma}{X_o}$, and dividing by ρ_e U_e we will get:

$$\eta_e-\eta_m=\int_s^e\frac{\rho}{\rho_e}\Phi d\eta \tag{3}$$

But, η_e and η_m for two-stream mixing can be converted from $\underline{\eta_e}$, $\underline{\eta_m}$ for single stream mixing such that:

$$\eta_e=\underline{\eta_e}\left(\frac{1-\Phi_B}{1+\Phi_B}\right)\ \eta_m=\underline{\eta_m}\left(\frac{1-\Phi_B}{1+\Phi_B}\right)$$

After substituting Eq. (3) into Eq. (2), following expression can be obtained for subsonic jet:

$$0=-\underline{\eta_e}\left(\frac{1-\Phi_B}{1+\Phi_B}\right)+\underline{\eta_m}\left(\frac{1-\Phi_B}{1+\Phi_B}\right)+\int_s^e\frac{\rho}{\rho_e}\Phi d\eta$$

For the supersonic jet,

$$0=-\underline{\eta'_{e'}}\left(\frac{1-\Phi'_B}{1+\Phi'_B}\right)+\underline{\eta'_{m'}}\left(\frac{1-\Phi'_B}{1+\Phi'_B}\right)+\int_{s'}^{e'}\frac{\rho'}{\rho'_{e'}}\Phi' d\eta'$$

Now, considering the momentum equation for the flow below the streamline e at the virtual origin ($x=0$) and downstream section at $x=X_0$:

$$\rho_eU_e^2(\underline{y_e}-\underline{y_m})=\int_{-\infty}^e\rho u^2dy$$

or

$$\underline{\eta_e}-\underline{\eta_m}=(1-Cr_e^2)J_{2e} \tag{4}$$

where

$$J_{2e}=\int_{-\infty}^e\frac{\Phi^2}{1-Cr_e^2\underline{\Phi^2}}d\eta$$

After comparing Eq. (1) and Eq. (4), one can find virtual distance X_o such as:

$$X_0=\frac{\sigma\delta_2}{(1-Cr_e^2)(J_{1e}-J_{2e})}$$

$$X_0'=\frac{\sigma'\delta_2'}{(1-Cr_{e'}^2)(J'_{1e'}-J'_{2e'})}$$

3. Balance

3.1 Mass balance

Figure 4 illustrates the mass conservations. The

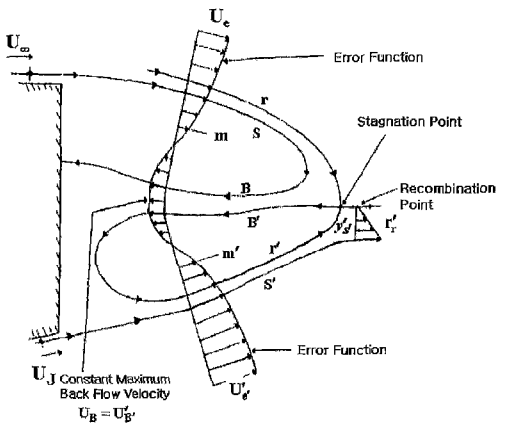

Fig. 4 Closed wake model

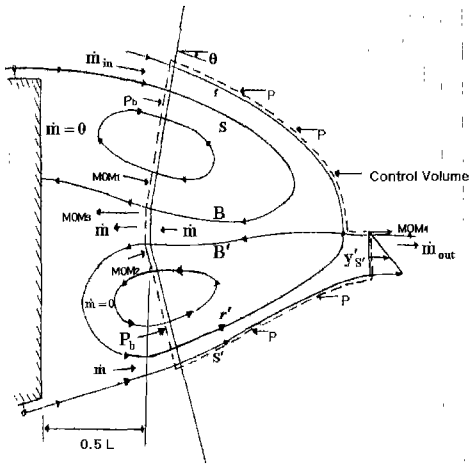

Fig. 5 Control volume for momentum and mass conservation

r and r' streamlines join at a saddle point at the end of the wake. Streamlines s and r form a corridor for the air which will be re-circulated to the base region, and then r' and s' streamlines conduct this mass from the base to the downstream atmosphere. In general, when two free jet surfaces join in this manner, the stronger flow (higher total pressure) is the ejector and the weaker is the feeder.

It is assumed that air is the gas in the corridor r-s, in the trapped vortex s-B, and in the corridor $B-B'$. From B to the jet exhaust stream, the gas is a mixture of air and engine exhaust gas. For the air regions, only T and P_0, vary across streamlines as functions of velocity Φ. For the mixed gas regions, T_0, γ and $\mathfrak{R}$ also vary with Φ'. The density ratio for the airflow region simplifies to

$$\frac{\rho}{\rho_e}=\frac{1-Cr_e^2}{1-Cr_e^2\Phi^2}$$

Mass conservations are:

$$2\pi\bar{R}_{r-s}\int_s^r \rho U dy=2\pi\bar{R}_{s'-r'}\int_{r'}^{s'} \rho' U' dy'$$
$$=2\pi\bar{R}_{B-B'}\int_{B'}^{B} \bar{\rho} U_B dy \qquad (5)$$

The bar indicates average value.
where

$$\bar{\rho}_B=\frac{1}{2}[\rho_B+\rho'_{B'}]$$
$$\bar{X}=X_0+0.5L$$
$$\bar{X}'=X_0'+0.5L$$

3.2 Momentum balance

The control volume for satisfying the momentum equation is shown in Fig. 5. The momentum equation is of the form.

$$\sum F_{Ax}=\sum m_{out}U_{Ax}-\sum \dot{m}_m U_{Ax}$$

where the subscript Ax means the axial direction. In the following development, θ is the angle between the streamline and the nacelle axis. Since the control volume is bounded by streamlines on the top and bottom in Fig. 5, these are four momentum terms:

Mom1: at mid wake between B and r
Mom2: at mid wake between B′ and s'
Mom3: at mid-wake between B and B′
Mom4: at downstream of wake between rr' and s'

The forces acting on the bubble are due to static pressure. Since both the streamlines r and s′, are close to the inviscid wake surfaces, an assumption is made that the static pressure does not vary from streamline to streamline. Also, in the inviscid analysis, the pressure was assumed to be a function of X direction only in the wake region. Therefore, the surface force acting in the axial direction on the bubble is calculated by summing up the surface pressures on the bubble surface geometry used in the potential flow calculation.

$$\sum F_{Ax}=\text{Mom1}+\text{Mom2}+\text{Mom3}+\text{Mom4} \qquad (6)$$

3.3 Energy balance

The control volume in Fig. 5 is also used for energy conservation computations. Energy transfer is done only by convection since the streamlines which boundaries have very small cross stream temperature gradients. All terms are of the form:

$$\dot{E}=\int h_o d\dot{m}$$

15

$$=\int \frac{\gamma \Re}{\gamma-1} T_o \rho U dy \text{ (energy/sec)} \qquad (7)$$

If the ΣE does not equal zero, $T_{oB'}$ is changed to satisfy the equation. The base temperature is then:

$$T_b=\frac{1}{2}(T_{oB}+T_{oB'})$$

4. Results and Discussion

Despite numerous inquires to research laboratories and engine manufacturers, no reliable data were found to test this method in all of its capabilities: axisymmetric, both subsonic and supersonic, and with engine exhaust gas at high temperature and different from air. Figures 6 to 11 show the predicted trends and the physical descriptions are provided as needed. The basic phenomenon is entrainment of air from the wake by the mass flux of the two streams. So values of $\rho_e u_e$ and $\rho'_{e'} u'_{e'}$ are the main criteria. Unless oth erwise listed, $M_\infty=0.6$, $M_j=1.4$, $\theta_j=10°$, $L/H=2.0$, $\gamma=1.31$, $\Re=70\frac{ft-lb}{lb_m R}$, and $T_{oJ}=3T_{0\infty}$.

Figure 6 shows the computed pressures with variable exhaust gas temperatures. It can be seen that the base pressure (P_b/P_∞) increases slightly with increasing jet stagnation temperature, mainly due to decreasing density. From this simple analysis, it is expected that there will be much more air entrainment when air properties are used instead of the gas properties, and subsequently higher mass flux will decrease the base pressure.

Figure 7 shows the computed pressures with variable flight Mach numbers. It can be observed that the base pressure decreases with increasing flight Mach number. Simple justification is as follows. An increase in M_∞ corresponds to an increase in velocity for constant atmospheric pressure and temperature. Therefore, it is expected that more air is entrained from the base region to the free stream and thus the higher mass flux at the base causes the base pressure to drop.

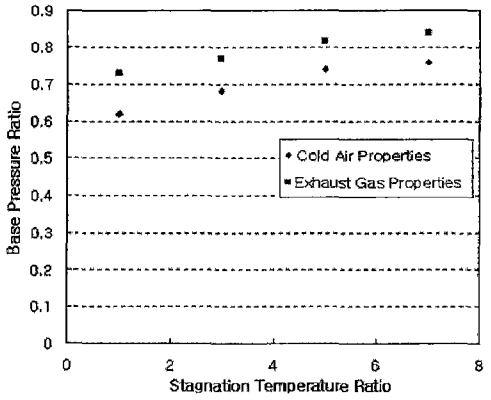

Fig. 6 Effect of stagnation temperature

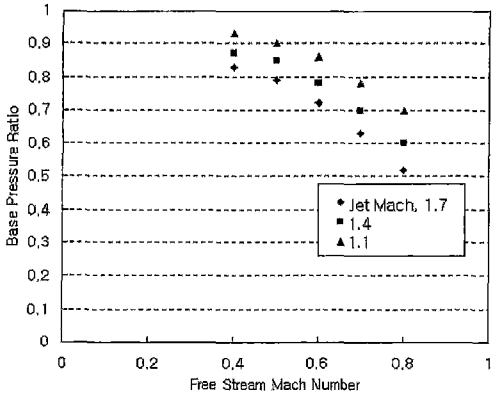

Fig. 7 Effect of flight Mach number

Figure 8 illustrates the computed base pressures with variable Jet Mach numbers. Note that the base pressure decreases with increasing jet Mach number. The following analytical argument is the same as for Fig. 7. In Fig. 6, it is interesting to compare the above results using the air properties instead of the exhaust gas properties.

In Fig. 6, it is demonstrated that change in the jet gas physical properties results in base pressure reduction of 12 %. We see that change of $T_{oJ}/T_{o\infty}$ from 3 to 1 for the gas reduces P_b by 8%. If wind tunnel simulation uses cold air as the exhaust gas, both of the simplifications may be made. Com-

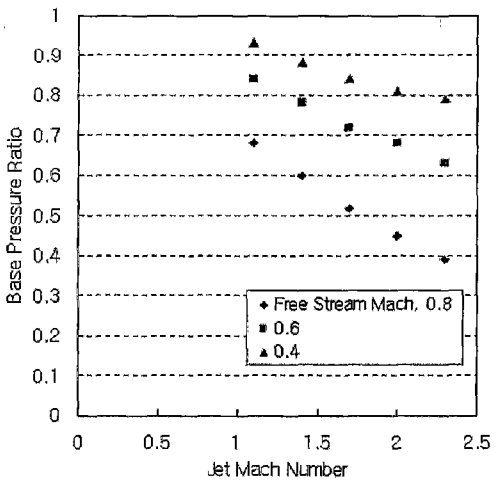

Fig. 8 Nozzle jet Mach number effect

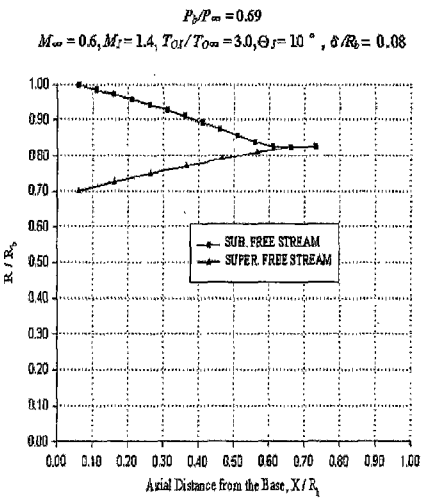

Fig. 9 Streamline shape for cylindrical nacelle(L/H=2.0)

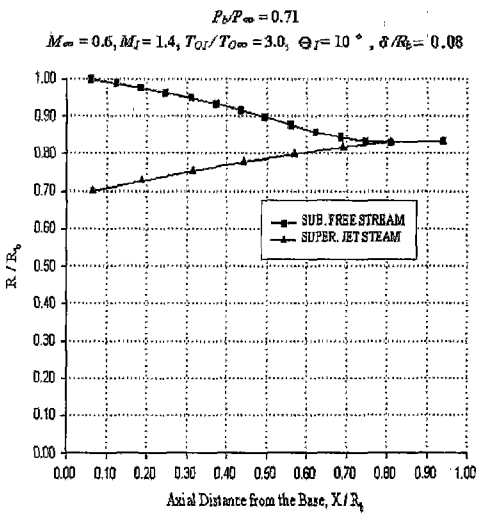

Fig. 10 Streamline shape for cylindrical nacelle(L/H=2.5)

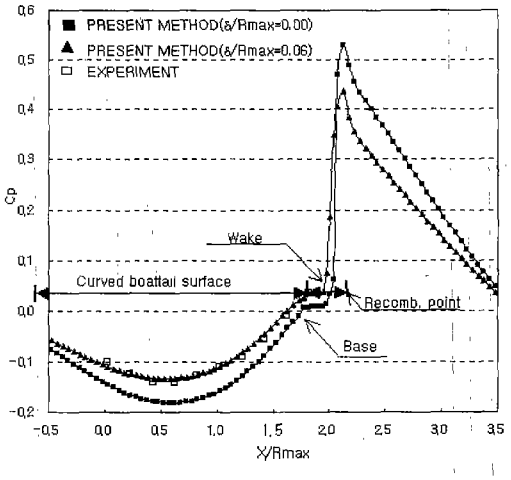

Fig. 11 Computed and experimental pressure on boattail wake (Peace, 1990)

putation of this condition gives P_b/P_∞=0.62, which is 20% reduction. This may be a warning for accepting such a simulation.

The wake length, L, is chosen at the beginning and seldom changed. Trial computations indicated that the wake length is not a sensitive parameter in this wake region (Fig. 9, 10). For L/H=2.0 and L/H=2.5, the base pressures (P_b/P_∞) are 0.69 and 0.71, respectively

Figure 11 shows the experimental and computed pressures for a boattailed nacelle tested in a wind tunnel with air in both streams and equal total temperatures on a circular arc boattail geometry. The afterbody pressure and base pressure are well predicted for this attached flow, especially if a reasonable boundary layer thickness is assumed. Figure 12 shows the streamline shape on the boattail wake.

5. Conclusions

An analytical method has been developed to predict the base flow for an axisymmetric blunt

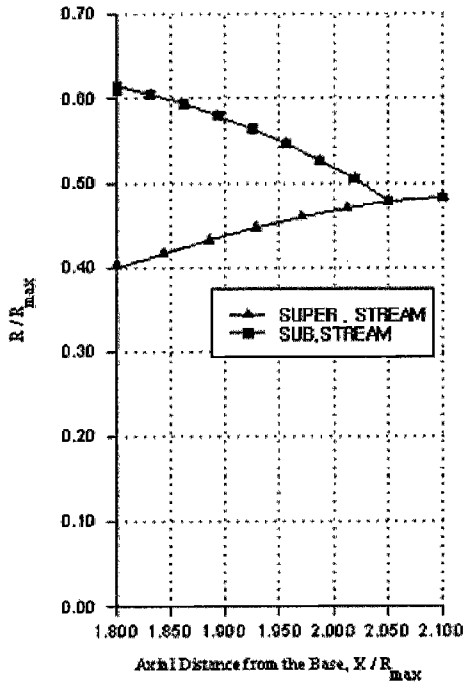

Fig. 12 Streamline Shape on Boattail Wake

body between subsonic and supersonic flows. A computational flow model has also been developed and validated against a limited amount of experimental data available with good agreement. However, no experimental data were found to include all of the relevant variables in this analysis. The lack of experimental data precludes complete testing of the present model. However, computed results show a qualitatively correct trend with the conditions such as the wake shape, velocities of the major streamlines, base pressure ratio and wake stagnation temperature as expected.

The computational time was between 25 and 35 minutes with IBM ES9121 computer at Wichita State University, Kansas. The program required modest computational time and capacity and should be useful in preliminary aircraft design calculations.

Recommendation for future work is to extend the model to include three different mixing streams by adding another airflow between the streams considered here. This would treat the fan-jet case or cooling air for an afterburner engine. This analytical method may be applied easily to a rocket engine nozzle having a large base area.

References

Diewert, G. S., 1980, "Numerical Simulation of Three-Dimensional Boattail Afterbody Flow Field," *AIAA* Paper 80~1347.

Dixon, R. J., and Page, R. H., 1970, "Turbulent Base Flow on an Axisymmetric Body with a Single Exhaust Jet," *J. of Aircraft*, Vol. 7, No. 7.

Hansen, G. A., 1982, "Navier-Stokes Solutions for an Axisymmetric Nozzle," *AIAA Journal* Vol. 20.

Hill, W. G. and Page, R. H., 1969, "Initial Development of Turbulent, Compressible Free Shear Layer," *J. of Basic Engineering (ASME)*, Vol. 91, Series D, No. 1.

Holst, T., 1977, "Numerical Simulation of Axisymmetric Boattail Fields with Plume Simulators," *AIAA* paper 77~224.

Izadi, M. J., 1991, "Computational Fluid Dynamics of the Base Flow on a Plane Body between a Subsonic Flow on One Side and a Supersonic Flow on the Other," Ph. D. Dissertation, Wichita State University.

Korst, H. H., 1956, "A Theory for Base Pressures in Transonic and Supersonic Flow," *J. of Applied Mechanics*, Vol. 23, No. 4.

Korst, H. H., and Tripp, W., 1957, "The Pressure on a Blunt Trailing Edge Separating Two Supersonic Two-Dimensional Air Streams of Different Mach Numbers and Stagnation Pressures, but Identical Stagnation Temperatures," *Proceedings of Fifth Midwestern Conference on Fluid Mechanics*, Univ. of Michigan.

Kuchemann, D., 1953, *Aerodynamics of Propulsion*, McGraw-hill Book Company, Inc, 1953, pp. 305~316.

Mikhail, A. G., 1978, "Computation of a Supersonic Flow Field Past an Axisymmetric Nozzle Boattail with Jet Exhaust," *AIAA* Paper 78~993.

Page, R. H., and Korst, H. H., 1955, "Nonisoenergetic Turbulent Compressible Jet Mixing with Consideration of its Influence on the

Base Pressure Problem," *Proceedings of Fourth Midwestern Conference on Fluid Mechanics*, Purdue Univ.

Peace, A. J., 1990, "Turbulent Flow Predictions for Afterbody/Nozzle Geometries Including Base Effects," *J. of Propulsion*, Vol. 7, No. 3.

Perry, K. M., and Forester, C. K., 1979, "Numerical Simulation of Multistream Nozzle Flows," *AIAA* Paper 79~1549.

Shapiro, A. H., 1953, *The Dynamics and thermodynamics of Compressible Fluid Flow*, Vol. 1, John Wiley & Sons Inc.